https://doi.org/10.5194/nhess-2021-218
Preprint. Discussion started: 21 July 2021

Natural Hazards and Earth System Sciences
Discussions

Comprehensive evaluation of hydrological drought and the effects of large reservoir on drought resistance in the Hun River basin, NE China

Fengtian Yang[1,2], Shupeng Yue[1,2] , Xiaodan Sheng[3]

[1] College of New Energy and Environment, Jilin University, Changchun 130021, China

[2] MOE Key Laboratory of Groundwater Resources and Environment, Jilin University, Changchun 130021 China

[3] Dahuofang Reservoir Authority of Liaoning Province Liability Company, Fushun 11300 China

Correspondence to: Shupeng Yue (yuesp_123@163.com)

Abstract. Evolution of drought under changing climate and the operation of large reservoir play an important role in drought warning and control. Thus, the evolution characteristics of hydrological drought and the effects of large reservoir on drought resistance are explored in the Hun river basin (HRB). Firstly, Standardized runoff Index (SRI) was adopted to evaluate the evolution characteristics of hydrological drought. Meanwhile, based on drought duration and severity identified by the run theory, the copula function with the highest goodness of fit was selected to calculate the return period of hydrological drought. Furthermore, the propagation time from meteorological to hydrological drought were determined by calculating the Pearson correlation coefficients between 1-month SRI and multi-time scale Standardized precipitation index (SPI). Finally, based on the cumulative precipitation deficit thresholds for triggering hydrological drought, the impact of large reservoir on drought resistance of the basin was revealed. The results show that: (1) hydrological drought showed a slight strengthening trend in the eastern, while presented alternate characteristics of drought and flood in the western and center of the HRB from 1967 to 2019; (2) the western and center of the HRB were vulnerable districts to hydrological drought with longer drought duration and higher severity; (3) the most severe drought with drought duration of 23 months, severity of 28.7, and corresponding return periods that both exceed the thresholds of duration and severity and exceed the threshold of duration or severity were 371 years and 89 years, respectively; (4) the propagation time from meteorological to hydrological drought of the lower reaches of large reservoir has been significantly prolonged owing to the operation of large reservoir; and (5) the operation of large reservoir strengthened the drought resistance in the lower reaches while lightly weaken in the upper reaches of large reservoir.

1 Introduction

Drought is a complex natural disaster caused by the abnormal decrease of precipitation, which has a grievous fatal effects on agriculture, ecology and social economy (Oladipo, 1985; Huang and Chou, 2008; Huang et al., 2015; Fang et al., 2019; Guo et al., 2019). Remarkable changes in global climate and environment aggravate the occurrence of hydrological extreme

https://doi.org/10.5194/nhess-2021-218
Preprint. Discussion started: 21 July 2021


Natural Hazards and Earth System Sciences Discussions

events characterized by drought (Wilhite and Glantz, 1985; Palmer and Räisänen, 2002; Kunkel, 2003; Beniston and Stephenson, 2004; Christensen and Christensen, 2004; Leng et al., 2015). Hydrological drought refers to the condition when the water level of a river or aquifer is lower than normal. The hydrological drought index based on runoff variation can reveal the hydrological drought status of the basin well (Mishra and Singh, 2011; Wang et al., 2020). SRI is commonly applied in hydrological drought monitoring and evaluation and has been widely used in drought frequency analysis and drought risk management (Vicente-Serrano et al., 2012; Rivera et al., 2017; Chen et al., 2018; Xu et al., 2019; Yang et al., 2020; Guo et al., 2020). Based on the drought index, the characteristics of drought events can be revealed quantitatively. Run theory, a time series analysis method, is widely applied to identify drought events and extract drought characteristic values, such as drought duration and severity (Kim et al., 2011; Liu et al., 2016a, 2016b; Wu et al., 2017; Sun et al., 2019). Copula function could better combine multiple drought characteristic variables and provides a valid way in multivariate frequency analysis (Mirabbasi, 2012; Lee et al., 2013; Vyver and Bergh 2018; Dash et al., 2019; Lindenschmidt and Rokaya, 2019). Therefore, based on drought duration and severity identified by the run theory, the copula function with the highest goodness of fit was selected to calculate the return period of hydrological drought (Kao and Govindaraju, 2009; Mirabbasi et al., 2012).

In general, hydrological drought is a response to the accumulation of meteorological drought conditions. The relationship between hydrological drought and meteorological drought has been discussed by many scholars and it is believed that the main element leading to hydrological drought is meteorological drought (Pandey and Ramasastri, 2001; Van Loon et al., 2012; Lorenzo-Lacruz et al., 2013; Leng et al., 2015; Barker et al., 2016; Gevaert et al., 2018; Sattar et al. 2019). However, what is the intensity of the meteorological drought that triggers hydrological drought with different levels has not yet clarified. In other words, it is to determine the trigger threshold of meteorological drought corresponding to hydrological drought at different levels. The exploration of the propagation time from meteorological drought to hydrological drought (PTMH) can enhance the understanding of the process of drought propagation. Meanwhile, drought propagation threshold can be applied to characterize drought resistance of watershed, with the higher the drought propagation threshold, the stronger the drought resistance (Guo et al., 2020). Therefore, a threshold model of drought propagation based on Bayesian network is established to realize the quantitative evaluation of the drought resistance of the catchment in this study.

Moreover, the runoff process downstream of the reservoir can be redistributed on the spatial and temporal scale through the operation of the reservoir (Shiklomanov et al., 2000; Chang et al., 2019; Wang et al., 2019; Guo et al., 2020). There are many researchers have revealed to some extent the influence of reservoirs operation on drought, especially on hydrological drought (Wu et al., 2016; Wu et al., 2018; Wang et al., 2019; Guo et al., 2020). However, the effects of large reservoir on drought propagation process and drought resistance of the catchment have not been clearly revealed. It is helpful to establish the warning and control system of hydrological drought to clarify the influence of large reservoirs on the drought resistance

https://doi.org/10.5194/nhess-2021-218
Preprint. Discussion started: 21 July 2021


Natural Hazards and Earth System Sciences Discussions

of watershed. Therefore, the effects of large reservoir on drought propagation and drought resistance of the catchment are discussed by calculating and analyzing the PTMH and the cumulative precipitation deficit (CPD, mm) in HRB.

In general, the primary objectives of this paper are: (1) to reveal the spatiotemporal evolution characteristics of hydrological drought; (2) to select the best-fit copula and calculate the hydrological drought return period; (3) to determine the PTMH; (4) to establish threshold model of drought propagation based on Bayesian network and quantitatively evaluate the influence of large reservoir on drought resistance.

2 Study region and data

The HRB, as presented in Fig. 1, is located in Liaoning Province, NE China and covers an area of 11,481 km^2, among which the hilly area occupies 67% and plain area 33%. The basin belongs to the temperate semi-humid and semi-arid monsoon climate, with four distinct seasons and the same season of rain and heat. The warm and wet air flow from the low latitude tropical monsoon circulation prevails in the summer brings more rainy days, while the Siberia-Mongolia high pressure dry cold continental air flow occurs during the winter, prevailing north wind and northwest wind, resulting in low temperature and less precipitation. The multi-year average precipitation is approximately 780 mm, with obvious seasonal characteristics, and the precipitation in the main flood season (July to August) accounts for about 48.5% of the annual precipitation.

Dahuofang (DHF) reservoir, located in Fushun city, Liaoning Province, is a large-scale water control project in the HRB, with a total storage capacity of 2.268 billion cubic meters. DHF reservoir plays a vital function in flood control and water supply, as well as for power generation and fish farming. Since the operation of DHF Reservoir in 1958, the agricultural irrigation, the river ecosystem of the region and the hydrological condition of the river channel have been greatly affected. Three hydrological stations in HRB were selected from upstream to downstream: Dahuofang (DHF), Shenyang (SY), and Xingjiawopeng (XJWP) stations to explore the spatial distribution of hydrological drought in this study. The three hydrological stations selected are located downstream of each basin, so the hydrological information of each basin can be reflected by the status of the corresponding hydrological stations (Fu et al., 2004). They represent the hydrological conditions of above DHF, DHF to SY and SY to XJWP, respectively. In addition, taking Beikouqian (BKQ) station in the upstream of DHF reservoir as a control, the effects of large reservoirs on drought propagation and drought resistance in the basin were discussed. The monthly runoff dates of these four hydrological stations and monthly precipitation data of the twenty meteorological stations during 1967–2019 were adopted in this study, which were collected from the Hydrological Data of Liao River Basin from the Year Book of Hydrology P.R.CHINA. Additionally, tyson polygon method was applied to calculate the precipitation of meteorological stations to get the corresponding area precipitation of each hydrological station.

https://doi.org/10.5194/nhess-2021-218
Preprint. Discussion started: 21 July 2021

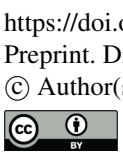

Natural Hazards and Earth System Sciences
Discussions

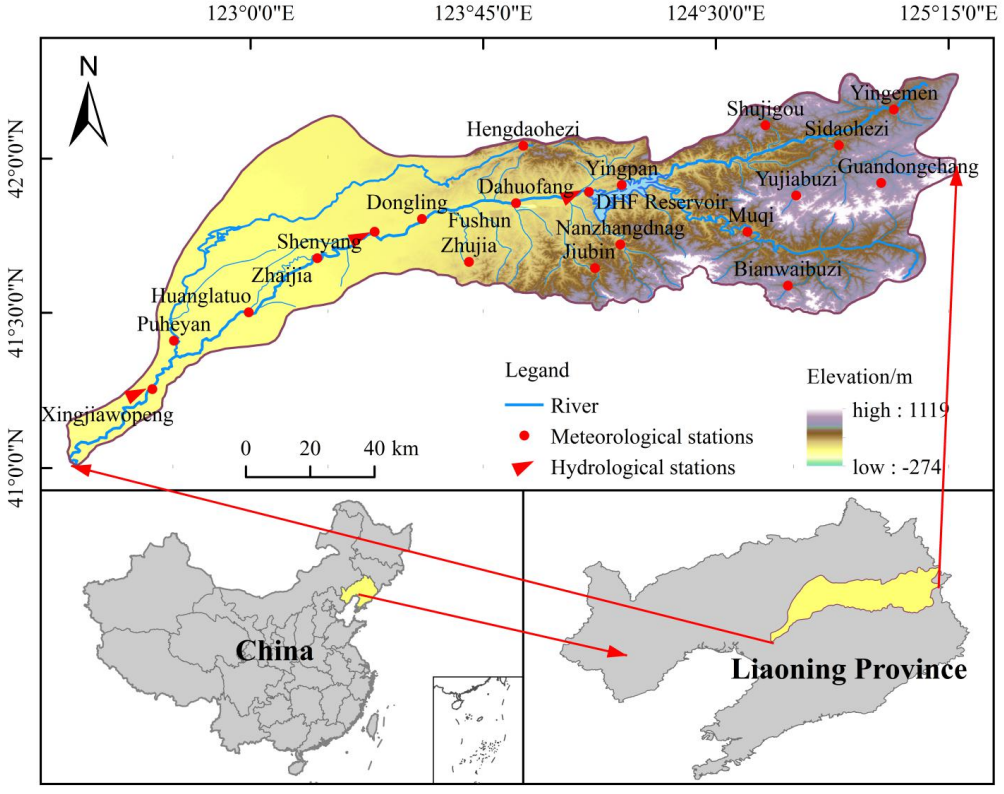

Figure. 1 Locations of the HRB, DHF reservoir, and the meteorological and hydrological stations.

Table. 1 Definition of drought conditions based on the SPI (SRI).

State	Condition	Criterion
1	Non-drought	SPI(SRI)>-0.5
2	Mild drought	-1.0<SPI(SRI)≤-0.5
3	Moderate drought	-1.5<SPI(SRI)≤-1.0
4	Severe drought	-2.0<SPI(SRI)≤-1.5
5	Extreme drought	SPI(SRI)≤-2.0

3.2 Run theory and copula functions

Run theory is a time series analysis method which is widely applied to identify drought events and extract drought characteristic values (Zhao et al., 2017; Sun et al., 2019). In this paper, based on the three thresholds SRI_0 (- 0.5), SRI_1 (- 1.0) and SRI_2 (0.0), the run theory was used to identify three drought factors, namely drought frequency, duration and severity, from the 1-month scale SRI sequence. Fig. 2 shows the process of drought recognition based on the threshold method, and the specific identification process is as follows:

(1) When the SRI value is less than SRI_0, it shows drought characteristics. From the time (t_1) when SRI value is less than or equal to SRI_0 to the time (t_2) when SRI value is greater than or equal to SRI_0, it is preliminarily recognized that a drought

https://doi.org/10.5194/nhess-2021-218
Preprint. Discussion started: 21 July 2021

Natural Hazards and Earth System Sciences
Discussions

has occurred. The total run length S is drought severity, and the run duration D (t_2-t_1) is drought duration. Fig. 2 contains five drought processes (a, b, c, d and e).

(2) On the basis of (1), if the drought duration of the drought process is one period (a, c) and its corresponding SRI value is less than SRI_1, it is considered that a drought event has occurred (a), otherwise it is defined as no drought event (c).

(3) If the time interval between two adjacent drought events (d, e) is one month, and the SRI value of this period is less than SRI_2, the two drought events are combined into one drought event, and drought severity is S=S_d+S_e, the drought duration is D=D_d+D_e+1, otherwise they are considered as two drought events.

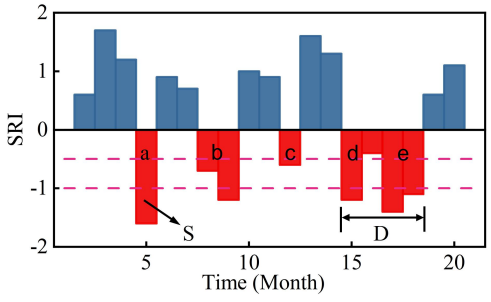

Figure.2 Drought identification process and definition of drought characteristic variables.

The sequence of drought duration and severity identified by the run theory were fitted by five common functions, including Gamma (GAM), Generalized extreme value (GEV), Exponential (EXP), Lognormal (Logn) and Weibull (WBL) distribution. Kolmogorov-Smirnov (K-S) test and AIC test were applied to determine the best-fit marginal distribution functions. Copula function, a multidimensional joint distribution function defined in [0,1], can integrate marginal distributions of several dependent random variables to structure a joint probability distribution with multiple features. Previous studies have proved that the copula function is an high-efficiency tool for multivariate probability analysis of drought (Hao and Singh, 2015; Salvadori and De Michele, 2015; Ren et al., 2020), its equation is expressed as follows:

$$C(u,v) = \varphi^{-1}\big(\varphi(u), \varphi(v)\big) \quad (1)$$

where $C(u,v)$ represents the copula function combining two random variables u and v; and φ is convex function.

The dependency structure between drought duration and severity were modeled by the commonly used binary copula functions, including Gumbel, Clayton, Frank, t and Normal copula (Wang et al., 2020). Root mean square error (RMSE) and AIC test were applied to select the highest goodness of fit best fitting good (GOF) copula function. Several joint probability expressions corresponding to bivariate return periods were used to further explore the occurrence frequency of hydrological drought. The expressions of joint probability are defined as:

$$T_{and} = \frac{E(L)}{P[(D>d \cap (S>s))]} = \frac{E(L)}{1-F_D(d)-F_S(s)+F(d,s)} \quad (2)$$

$$T_{or} = \frac{E(L)}{P[(D>d) \cup (S>s)]} = \frac{E(L)}{1-F(d,s)} \quad (3)$$

https://doi.org/10.5194/nhess-2021-218
Preprint. Discussion started: 21 July 2021

Natural Hazards and Earth System Sciences Discussions

where $E(L)$ denotes the expected value of drought interval and $F_D(d)$ and $F_S(s)$ are marginal cumulative density function of drought duration and severity, respectively. T_{and} is the return period of drought events that both exceed the thresholds of duration ($D \geq d$) and severity ($S \geq s$) and T_{or} is return period of drought events that considered exceed the threshold of duration ($D \geq d$) or severity ($S \geq s$).

3.3 The drought propagation time

In general, hydrological drought is a response to the accumulation of meteorological drought conditions. Since the change of hydrological regime can be characterized sensitively by the single time scale SRI, and the accumulation of meteorological drought in the previous n months can be reflected by the n time scale SPI, the time scale of SPI with the highest correlation with the single time scale SRI is regarded as PTMH (Barker et al., 2016; Huang et al., 2017; Fang et al., 2020). In this study, the PTMH T_P was determined by calculating the Pearson correlation coefficient between the monthly scale SRI and the multi-time scale SPI(1-24 months).

3.4 The calculation of drought propagation threshold

Bayesian network, a probabilistic graph model, is widely used in drought impact assessment (Sattar et al., 2019; Guo et al., 2020). Therefore, a threshold model of drought propagation based on Bayesian network is established in this study. Suppose $X(x_1,x_2\ldots,x_n)$ and $Y(y_1,y_2\ldots,y_n)$ are two random variables, with X and Y as conditions and targets respectively. Then, in the case of $X \geq u$, the probability of $Y \geq v$ can be expressed as:

$$P(Y \geq v|X \geq u) = \frac{P(X \geq u, Y \geq v)}{P(X \geq u)} = \frac{1-x(u)-y(v)+C(x(u),y(v))}{1-x(u)} \quad (4)$$

where $C(x(u), y(v))$ represents the joint cumulative probability of $X \leq u$ and $Y \leq v$; $x(u)$ and $y(v)$ denote the cumulative probability of $X \leq u$ and $Y \leq v$; x and y are the marginal cumulative distribution of two random variable X and Y.

In this study, the hydrological drought characteristics (drought duration and severity) of each drought event are taken as the target, respectively, and the corresponding cumulative precipitation deficit (CPD, mm) is identified as the condition. The conditional probability of hydrological drought under different CPD conditions would be calculated. Based on the recognition of hydrological drought event by the run theory, the CPD of each drought event is calculated during the PTMH. The CPD is defined as:

$$CPD_n = -\left(\max_{D \geq t \geq 1} \sum_{i=t-T_P+1}^{t} (P_i - \overline{P}_m) + \sum_{i=1}^{D-t} (P_i - \overline{P}_m)\right) \quad (5)$$

where CPD_n is the corresponding CPD for the nth drought; P_i denotes the precipitation during the period of i; P_m represents the average precipitation of the mth month.

According to the method of determining the marginal distribution described in Section 3.3, GAM, EXP, GEV, Logn and WBL distributions were applied to fit the CPD. The commonly used bivariate theoretical copula functions, including Clayton, Frank, and Gumbel copula were considered for modeling the dependence structure between CPD and drought duration and

https://doi.org/10.5194/nhess-2021-218
Preprint. Discussion started: 21 July 2021


Natural Hazards and Earth System Sciences Discussions

severity, respectively, and the GOF copula functions were tested based on RMSE and AIC. In this study, the CPD corresponding to the confidence level of 0.95 was taken as the drought propagation threshold for triggering hydrological drought events, and this CPD threshold was used to characterize the drought resistance of the basin. In addition, the interval conditional probability is calculated in this model to further investigate the sensitivity of hydrological drought responding to different CPDs:

$$P(Y \geq v | u_1 \leq X \leq u_2) = \frac{P(Y \geq v, u_1 \leq X \leq u_2)}{u_1 \leq X \leq u_2} = \frac{x(u_2) - x(u_1) - C(x(u_2), y(v)) + C(x(u_1), y(v))}{x(u_2) - x(u_1)}$$

$$= 1 - \frac{C(x(u_2), y(v)) - C(x(u_1), y(v))}{x(u_2) - x(u_1)} \quad (6)$$

where u_1 and u_2 are the upper and lower limits of the given interval.

4 Results and discussions

4.1 Change trends of hydrological drought

Fig. 3 depicts the temporal variation trend of hydrological drought based on the monthly scale SRI in HRB from 1967 to 2019, which presented difference temporal evolution characteristics in each sub-basin. It is clear from Fig. 3a that the SRI sequence showed an non-significant decreasing trend in the DHF, which indicated that the drought showed slight strengthening trend in DHF. The significant strengthening trend of drought occurred from March 1991 to September 2004, with average SRI value of -0.54 and minimum of -3.33. Fig. 3 (b,c) presents that the temporal evolution characteristics of hydrological drought were similar in SY and XJWP, showed alternate characteristics of drought and flood. Droughts occurred mainly from May 1977 to April 1984, November 1988 to November 1993 and May 2000 to September 2003 in SY, with average SRI value of -0.84, -0.56 and -0.70, respectively. Similarly, droughts occurred mainly from April 1978 to May 1985, November 1988 to July 1993 and March 2000 to March 2005 in XJWP, with average SRI value of -0.57, -0.50 and -0.81, respectively.

In view of the multi-time scale characteristics of SRI, the seasonal scale SRI was calculated to analyze the seasonal variation trend of hydrological drought. Fig. 4 presents the temporal variation of hydrological drought at seasonal scales in HRB from 1967 to 2019. From the interannual perspective, the drought trend were different in sub-regions, with the linear slope of SRI changed from −0.089/10a to 0.469/10a. SRI showed a decreasing trend at spring, summer and autumn in DHF, with the linear slope of SRI were −0.025/10a, −0.008/10a and −0.050/10a, which indicated that drought was aggravating at spring, summer and autumn. The linear slope of SRI were 0.167/10a and 0.207/10a at spring and winter, while −0.054/10a and −0.079/10a at summer and autumn in SY, indicating that drought was strengthening in summer and autumn and decreasing in spring and winter. Similar to the temporal characteristics of SY, drought showed an strengthening trend in summer and autumn, while a decreasing trend in spring and winter in XJWP with the linear slope of SRI were −0.083/10a,

https://doi.org/10.5194/nhess-2021-218
Preprint. Discussion started: 21 July 2021

Natural Hazards and Earth System Sciences
Discussions

−0.089/10a, 0.319/10a and 0.469/10a, respectively. Moreover, it can be observed from Fig. 4 that both continuous drought and drought-flood abrupt alternation may occur in HRB within the year.

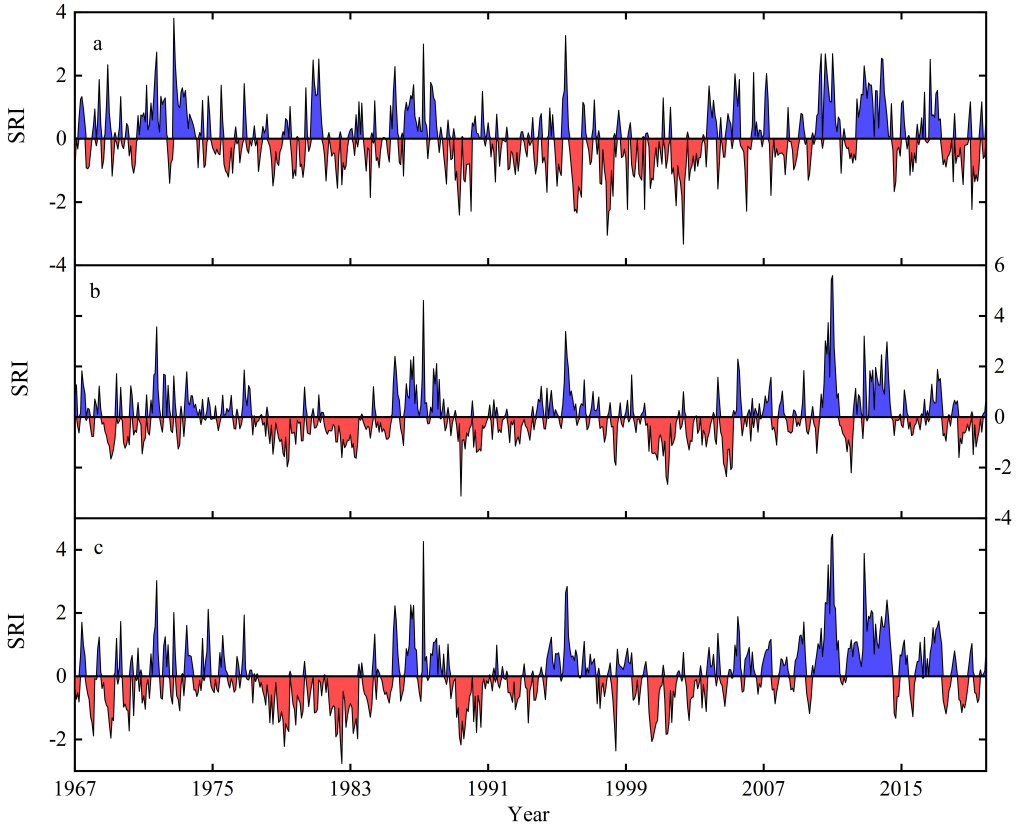

Figure.3 Temporal variation of hydrological drought based on monthly scales in HRB during 1967- 2019. (a)-(c) denote DHF, SY and XWP, respectively.

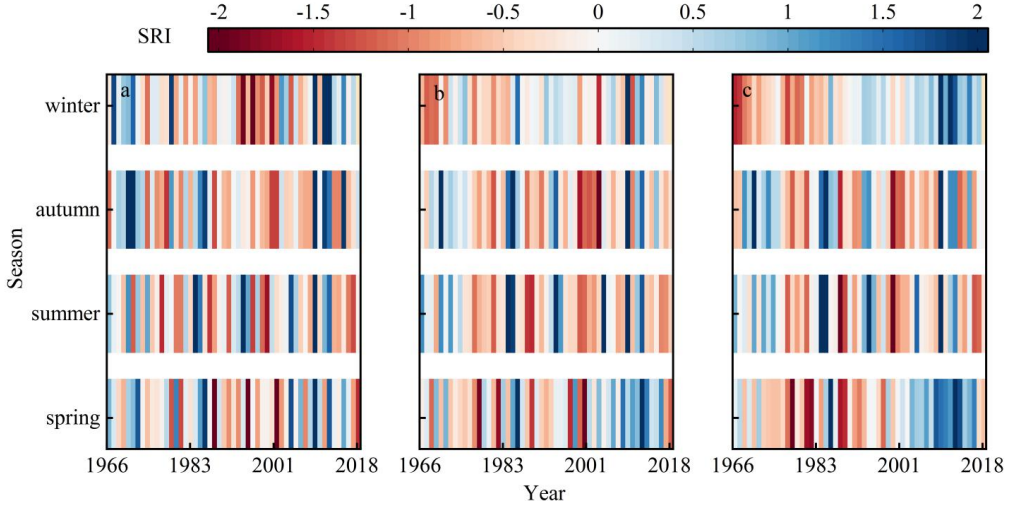

https://doi.org/10.5194/nhess-2021-218
Preprint. Discussion started: 21 July 2021

Natural Hazards and Earth System Sciences Discussions

Figure. 4 Heat map of hydrological drought at seasonal scales in the HRB from 1967 to 2019. (a)-(c) denote DHF, SY and XWP, respectively.

In order to further explore the temporal evolution characteristics of hydrological drought, the trend characteristic *U* value of M-K trend test were calculated. Table 2 shows the trend characteristic value *U* at the seasonal and annual scales. It is clear from Table 2 that the characteristics of drought trends in different periods and stations are obviously different. On the annual scale, the *U* value of DHF, SY and XJWP stations were −0.83, -0.37 and -0.09, indicating an non-significant strengthening trend of drought in the HRB. On the seasonal scale, the *U* values of each sub-basin in summer and autumn were less than zero, which indicated that drought was strengthening in summer and autumn in HRB. The *U* values of DHF were less than zero in spring and winter, which indicated that drought showed an strengthening trend in spring and winter at DHF. However, the *U* values of SY and XJWP stations were 2.15, 2.34, 3.67 and 6.64 in spring and winter, respectively. These trend characteristic *U* values passed the significance test of $\alpha = 0.05$, indicated that the drought showed a significant decreasing trend in spring and winter at the SY and XJWP of HRB. All in all, the drought at DHF showed an strengthening in all seasons and showed an strengthening trend in summer and autumn, while an decreasing trend in spring and winter at SY and XJWP, which can be confirmed with the conclusions of previous section.

Table. 2 *U* values of SRI in the HRB during 1967-2019.

Zone	DHF		SY		XJWP	
	U value	Trend	U value	Trend	U value	Trend
Spring	-0.52	downward	**2.15**	upward	**3.67**	upward
Summer	-0.40	downward	-1.47	downward	-1.49	downward
Autumn	-0.95	downward	-1.46	downward	-1.15	downward
Winter	-0.11	downward	**2.34**	upward	**6.64**	upward
Year	-0.84	downward	-0.37	downward	-0.09	downward

The bold letters denote that the *U* values passed the MK trend test of $\alpha = 0.05$.

Based on the run theory, three drought factors, namely drought frequency, duration and severity, were identified from the 1-month scale SRI sequence. Drought events which were detected sum up to 133 in 3 districts of HRB during 1967-2019. DHF was most frequently affected by drought, with a total of 57 drought events, followed by XJWP and SY with 39 and 37 drought events, respectively. The box chart of drought duration and severity was drawn, and the spatial distribution of drought was discussed (Fig. 5). Fig. 5 shows that districts with the mean of drought duration more than 5 months included SY and XJWP, while the median drought duration of XJWP was greater than DHF and SY. Besides, SY and XJWP have experienced extremely long duration drought events lasting more than 23 months. The districts in the wast (XJWP) and center (SY) were more likely experience longer drought events and the longer-duration drought events was most likely to occur in central regions. Drought severity and drought duration maintained a highly consistency. The highest drought severity occurred in XJWP and the mean drought severity of DHF was less than XJWP and SY (Fig. 5). In summary, western and center of the HRB were vulnerable district to hydrological drought, where the drought duration and severity

https://doi.org/10.5194/nhess-2021-218
Preprint. Discussion started: 21 July 2021

Natural Hazards and Earth System Sciences
Discussions
Open Access
EGU

were more serious than in eastern (DHF) districts. Nevertheless, the eastern region of the HRB was more sensitive to short-duration drought, which were dominated by two-month and three-month drought events.

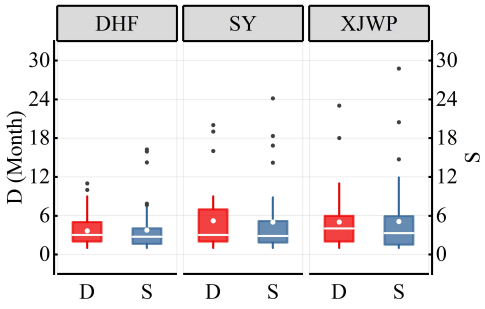

Figure.5 Box chart of duration and severity of hydrological drought.

4.2 Periodicity analysis

In this study, five common functions including Gamma, EXP, GEV, Logn, and WBL, were used to fit the sequence of duration and severity of hydrological drought events in the three sub-basins in the HRB and AIC and K-S test were applied to select the best-fit distribution, and the consequences were shown in Table 3. Table 3 illustrates that all of the optimal distributions passed the K-S test of $\alpha = 0.01$. The joint distribution of drought duration and severity was determined using the copula functions in the HRB. Based on the RMSE and AIC, the GOF copula functions were selected in the HRB (Table 4) .

Table. 3 Determination of the optimum marginal distribution function of drought characteristics.

Zone	Drought characteristics	Optimal distribution	AIC	K-S
BKQ	Duration	EXP	-283.37	0.190*
	Severity	Logn	-310.04	0.123*
	CPD	GAM	-374.31	0.062*
DHF	Duration	EXP	-333.89	0.094*
	Severity	GEV	-386.58	0.072*
	CPD	WBL	-404.90	0.061*
SY	Duration	EXP	-204.75	0.148*
	Severity	GEV	-249.64	0.098*
	CPD	GEV	-239.90	0.098*
XJWP	Duration	GEV	-239.43	0.105*
	Severity	Logn	-251.49	0.106*
	CPD	GEV	-236.55	0.113*

"*" denote that the optimal distribution passed the K-S test of $\alpha = 0.01$.

Table. 4 GOF evaluation of different copula functions about drought duration and severity in the HRB.

Zone	Clayton-copula		Gumbel-copula		Frank-copula		Normal-copula		t-copula	
	RMSE	AIC	RMSE	AIC	RMSE	AIC	RMSE	AIC	RMSE	AIC
DHF	0.05	-340.68	**0.04**	**-375.08**	0.04	-363.30	0.04	-371.35	0.04	-372.16
SY	0.04	-229.56	0.04	-238.93	**0.04**	**-245.28**	0.04	-241.23	0.04	-238.74
XJWP	**0.05**	**-237.35**	0.05	-231.59	0.05	-235.26	0.05	-235.51	0.05	-235.60

Bold letters represent the optimal copula functions.

https://doi.org/10.5194/nhess-2021-218
Preprint. Discussion started: 21 July 2021

Natural Hazards and Earth System Sciences
Discussions

Fig. 6 shows the contour plots of return period levels of drought events based on the optimal copula, and the return period T_{and} and T_{or} of drought events in each sub-basin can be observed. The drought return period increased with the increase of drought duration and severity in the HRB. For the same drought event, return period T_{and} would be higher than T_{or}. Meanwhile, regarding the same return period, drought duration and severity from large to small were SY, DHF and XJWP, respectively. In DHF, the drought occurred from September 2001 to July 2002 was the most severe, lasting 11 months, with severity of 16.2, and return period T_{and} and T_{or} were 33 years and 17 years, respectively. In SY, the most severe drought happened from May 2000 to November 2001, lasting19 months, with severity of 24.1, and return period T_{and} and T_{or} were 152 years and 24 years, respectively. Similarly, the drought occurred from August 1981 to June 1983 was the most severe in XJWP, lasting 23 months, with severity of 28.7, and return period T_{and} and T_{or} were 371 years and 89 years, respectively.

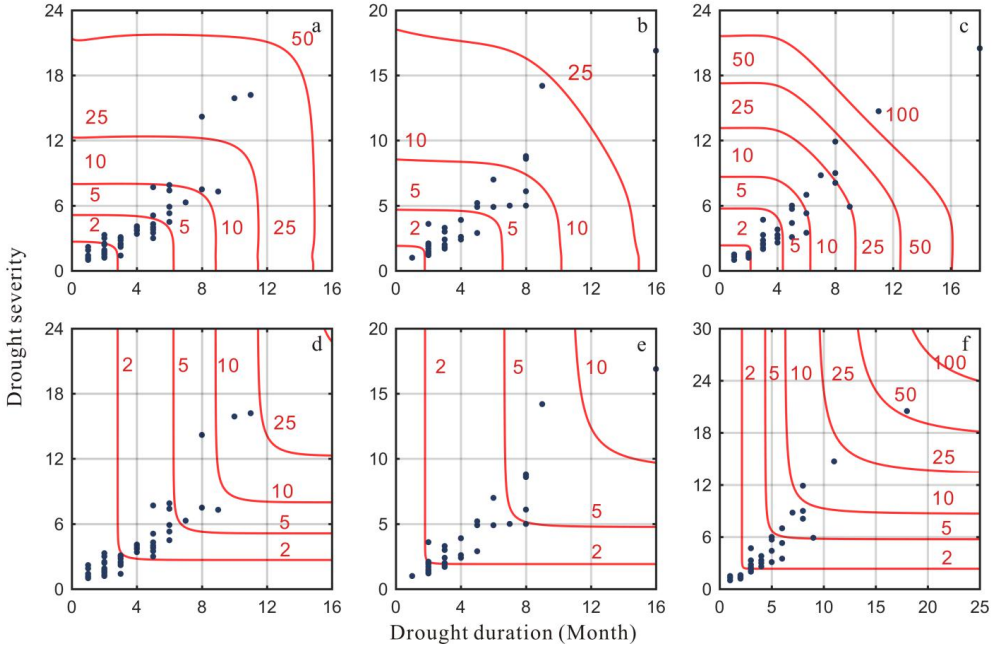

Figure. 6 The return periods T_{and} and T_{or} of 1-month scale drought events in DHF (a and d), SY (b and e) and XJWP (c and f).

Besides, according to the univariate empirical frequency of drought duration and severity, three typical drought scenarios were selected to analyze the return periods. The scenarios corresponding to the empirical frequency of 0.50, 0.25 and 0.05 of the univariate were defined as moderate, severe and extreme drought. Table 5 exhibits the drought return periods T_{and} and T_{or} under different drought scenarios and their corresponding drought duration and drought severity in DHF, SY and XJWP. For moderate drought, the return period T_{and} and T_{or} had the same regularity in DHF, SY and XJWP, with the largest value in SY, followed by XJWP and DHF. As for severe drought, the distribution of T_{and} and T_{or} about severe and extreme drought were consistent in DHF, SY and XJWP, which showed that SY has the highest return period T_{or}, followed by XJWP and DHF, while the return period T_{and} in XJWP was greater than SY and DHF. It should be noted that the drought presented the

https://doi.org/10.5194/nhess-2021-218
Preprint. Discussion started: 21 July 2021

characteristics of smaller return period with high drought duration and large severity in eastern of the HRB. It is foreseeable that eastern districts will be more likely to suffer from more serious drought events.

Table. 5 The drought return periods T_{and} and T_{or} under different drought scenarios and their corresponding drought factors in HRB.

Zone	Drought scenario	T_{and} (Year)	T_{or} (Year)	Drought duration	Drought severity
DHF	Moderate drought	2.3	1.7	3	2.6
	Severe drought	4.5	3.1	5	4.3
	Extreme drought	22.8	14.9	11	11.9
SY	Moderate drought	3.3	2.7	4	2.8
	Severe drought	6.7	4.8	7	5.3
	Extreme drought	71	18.6	16	20.7
XJWP	Moderate drought	3.2	2.6	4	3.5
	Severe drought	7.3	4.4	6	6.1
	Extreme drought	79	16.3	13	13.8

4.3 The propagation from meteorological to hydrological drought

Based on the superiority of SPI that it can be calculated at multi-time scales, the PTMH were determined by calculating the Poisson correlation coefficient between the monthly SRI and the multi-time SPI. The PTMH was indicated by the month with the strongest correlation. The Poisson correlation coefficient and the PTMH of four hydrological stations in HRB were shown in Fig. 7. It can be observed from Fig. 7 that the PTMH in HRB had obviously seasonal characteristics. The high correlation coefficients were mainly concentrated in spring and summer, and the corresponding PTMH ranged from 3 to 7 months, while the correlation coefficients were lower in autumn and winter with PTMH ranged from 2 to 5 months at BKQ and DHF. Nevertheless, high correlation coefficients were concentrated from late summer to early winter, and the corresponding PTMH ranged from 3 to 14 months, while the correlation coefficients were lower from late winter to early summer with PTMH ranged from 4 to 23 months at BKQ and DHF. It can be seen from Fig. 7 that the PTMH at SY and XJWP were significantly higher than at BKQ and DHF, which is likely that the operation of DHF reservoir has markedly effect the PTMH of the HRB.

https://doi.org/10.5194/nhess-2021-218
Preprint. Discussion started: 21 July 2021

Natural Hazards and Earth System Sciences
Discussions

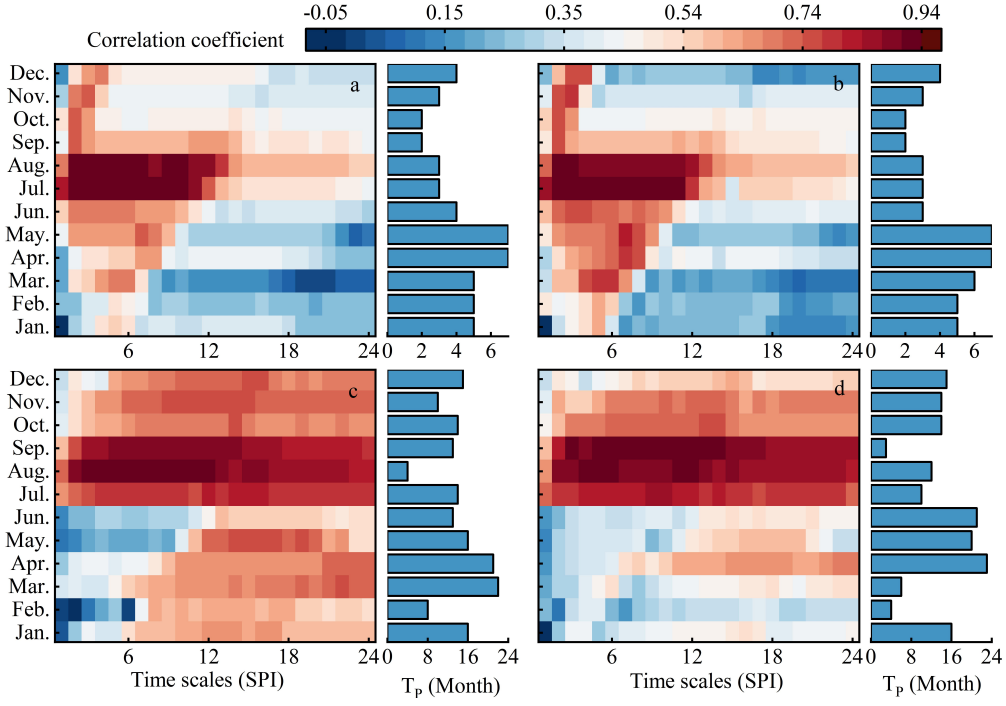

Figure. 7 The correlation between monthly SRI and multi-time scale SPI and the PTMH in BKQ (a), DHF (b), SY (c) and XJWP (d).

The detailed effects of DHF reservoir operation on the PTMH were revealed by calculating the PTMH of different periods. Fig. 8 expresses the results of the PTMH included the four seasons, water supply period (WS-P), storage period (S-P), and full series (F-series) at the four stations in the HRB. Considering the lack of data before the construction of the DHF reservoir, this paper holds that the consistency of PTMH was perfect before the construction of the DHF reservoir in the HRB and the status of BKQ station in the upstream of the DHF reservoir is considered as that before the construction of the DHF reservoir to analyze the effect of the reservoir operation on the propagation duration. The locations of the four hydrological stations are shown in Fig. 1. The BKQ station is located upstream of the DHF reservoir, while SY and XJWP stations are successively arranged in the downstream of DHF reservoir.

It is clear from Fig. 8 that, from the point of view of the F-series, the PTMH of SY (14.9 months) and XJWP (11.9 months) station were obviously higher than the BKQ (4.1 months) station's, whilst the PTMH of DHF (4.3 months) station was almost equal to BKQ station's, which indicated that the PTMH was significantly postponed by the operation of DHF reservoir. It signified that the operation of DHF reservoir has observably enhanced the drought resistance of the HRB. Moreover, the PTMH of SY station was higher than the XJWP station's, which implied that the improvement effect is weakness with the rising of the interval from hydrological stations to DHF reservoir. Similar to the F-series, the drought propagation times of SY and XJWP station were obviously higher than the BKQ station's from seasonal perspective, while the PTMH of DHF station was not significantly different from that of BKQ station. Meanwhile, the seasonal variations of

https://doi.org/10.5194/nhess-2021-218
Preprint. Discussion started: 21 July 2021

PTMH in DHF, SY, and XJWP station were brought into line with BKQ hydrological station with the characteristics of long PTMH in spring and winter, and short in summer and autumn, which shown that the construction of DHF reservoirs did not affect the seasonal distribution of drought propagation time. Higher temperatures in summer and autumn may be the reason for the relatively low PTMH of spring and winter. In addition, there are a large amount of snow in winter and most of the snow melts in the next spring at HRB. Therefore, the longer PTMH in winter and spring may be caused by the lower temperature in spring and winter and the melting of snow in spring. However, it is worth mentioning that compared with other seasons, the PTMH of XJWP station was longer than that of SY station in summer and compared to other stations, the PTMH of XJWP station in summer are longer than that of winter. These two changes indicated that the duration of drought propagation at XJWP in summer was prolonged, which may be due to the partial agricultural water supply from DHF reservoir directly reaching downstream through channels without passing through SY station in summer. For S-P, the drought propagation times of SY station and XJWP station were both longer than BKQ station, and with the rising of interval between hydrological station and DHF reservoir, the PTMH showed a decreasing trend, which showed similar characteristics with the F-series. It is worth mentioning that the PTMH of XJWP station is longer than SY station during WS-P, which was inconsistent with the conclusion that the PTMH decreases as the increase of the interval between hydrological station and reservoir during S-P. The reason for this is most likely that part of agricultural water supply from DHF reservoir directly reaching downstream through channels without passing through SY station, which increased runoff at XJWP station while SY station runoff was not affected. Moreover, agricultural water supplies mostly occur in the summer, which can be mutually verified with the results of seasonal perspective.

In conclusion, the PTMH of SY and XJWP station were higher than BKQ station's in different periods. The drought PTMH of the lower reaches of DHF reservoir has been remarkably strengthened in each period owing to the operation of DHF. Moreover, with the strengthening of hydrological drought level and the rising of interval between hydrological station and DHF reservoir, the improvement effect was weakened. Meanwhile, the PTMH showed longer in spring and winter, while shorter in summer and autumn and the PTMH of XJWP station was longer than that of SY station in WS-P because of the effect of agricultural water supply operation of DHF reservoir.

https://doi.org/10.5194/nhess-2021-218
Preprint. Discussion started: 21 July 2021

Natural Hazards and Earth System Sciences
Discussions

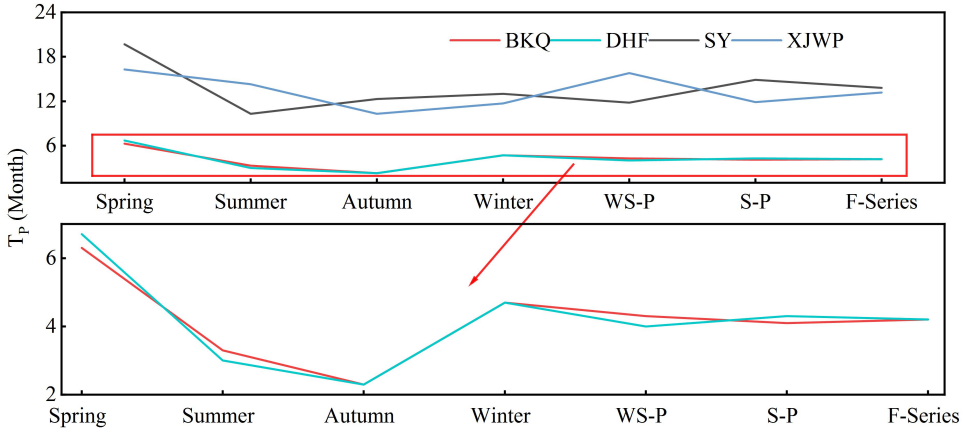

Figure. 8 The PTMH of BKQ, DHF, SY and XJWP from meteorological to hydrological drought in different periods.

4.4 The contribution of large reservoir to drought resistance of catchment

In this study, drought propagation threshold model was established to explore the influence of large reservoir on drought resistance of watershed. In the model, moderate, severe and extreme hydrological droughts defined in Section 4.2 were selected as specific hydrological droughts. The drought duration and severity of each hydrological drought event were taken as the target respectively, and the corresponding CPD was regarded as the condition. The CPD interval, triggering moderate, severe, and extreme hydrological droughts at a confidence level of 0.95, was calculated according to the drought propagation threshold model introduced in Section 3.5.

In this model, five common functions including Gamma, EXP, GEV, Logn, and WBL, were used to fit the sequence of CPD of hydrological drought events in the three sub-basins in the HRB and AIC and K-S test were applied to select the best-fit distribution, and the consequences were shown in Table 3. The commonly used bivariate theoretical copula functions, including Clayton, Frank, and Gumbel copula were considered for modeling the dependence structure between CPD and drought duration (D-CPD) and severity (S-CPD), respectively. Based on the RMSE and AIC, the GOF Copula functions were selected and shown in Table 6.

Table. 6 GOF evaluation of different copula functions between CPD and drought duration and severity at four stations.

Zone		Clayton-copula		Gumbel-copula		Frank-copula	
		RMSE	AIC	RMSE	AIC	RMSE	AIC
BKQ	D - CPD	0.04	-328.89	**0.03**	**-357.89**	0.04	-351.42
	S - CPD	0.04	-350.47	0.04	-345.27	**0.03**	**-356.09**
DHF	D - CPD	0.05	-329.21	**0.04**	**-363.87**	0.04	-356.69
	S - CPD	0.03	-415.23	0.03	-403.56	**0.02**	**-422.79**
SY	D - CPD	0.08	-186.73	**0.06**	**-202.51**	0.07	-199.87
	S - CPD	0.06	-208.39	**0.05**	**-239.79**	0.05	-234.15
XJWP	D - CPD	0.04	-243.17	0.04	-242.58	**0.04**	**-246.92**
	S - CPD	0.04	-247.25	0.04	-258.98	**0.03**	**-264.62**

https://doi.org/10.5194/nhess-2021-218
Preprint. Discussion started: 21 July 2021

The bold letters represent the selected optimal copula functions.

Fig. 9 shows the conditional probabilities of occurrence of hydrological droughts with different levels under the condition of various CPD in four stations. After the operation of DHF Reservoir, the CPD interval triggering different levels of hydrological drought and the improvement of drought resistance (IDR) were shown in Table 7. It can be seen from Table 7 that, in general, CPD intervals which triggered moderate, severe and extreme hydrological droughts in BKQ were lower than SY and XJWP, while higher than that of DHF, which signified that the operation of DHF reservoir has remarkably strengthened the drought resistance in the lower reaches of DHF reservoir while weakened the drought resistance in the upper reaches of DHF reservoir. Moreover, it was clear from Table 7 that, the IDR decline with the rising of hydrological drought level in DHF, which indicated that the weakening effect of drought resistance increased with the rising of hydrological drought level. On the contrary, the improvement effect of drought resistance increased with the rising of hydrological drought level in SY. With the increase of hydrological drought level, the IDR value of XJWP first increased and then decreased, and reached the maximum at severe drought level, which showed that the improvement effect of drought resistance was the greatest at severe hydrological drought level. Meanwhile, it was obvious from Table 7 that, the CPD and IDR showed an strengthening trend in moderate and severe drought levels, and a decreasing trend in extreme drought levels with the rising of interval between hydrological stations and DHF reservoir in the lower reaches of DHF reservoir. The results demonstrated that the improvement of drought resistance increased in moderate and severe hydrological droughts, while decreased in extreme hydrological droughts as the rising of interval between hydrological stations and DHF reservoir.

Table. 7 CPD threshold ranges for triggering different levels of hydrological drought at HRB.

Drought scenario		Moderate	Severe	Extreme
BKQ	CPD (mm)	[158.6,185.5]	[210.4,261.5]	[300.8,347.7]
DHF	CPD (mm)	[156.9,182.7]	[187.1,198.4]	[206.6,291.7]
	IDR (%)	[-0.8,-0.6]	[-18.1,-7.7]	[-31.3,-16.1]
SY	CPD (mm)	[204.3,218.0]	[290.6,314.6]	[493.1,543.5]
	IDR (%)	[9.3,15.2]	[15.3,26.7]	[56.3,63.9]
XJWP	CPD (mm)	[220.5,241.2]	[296.7,334.3]	[385.7,396.8]
	IDR (%)	[16.0,20.6]	[20.9,28.7]	[14.1,28.2]

https://doi.org/10.5194/nhess-2021-218
Preprint. Discussion started: 21 July 2021

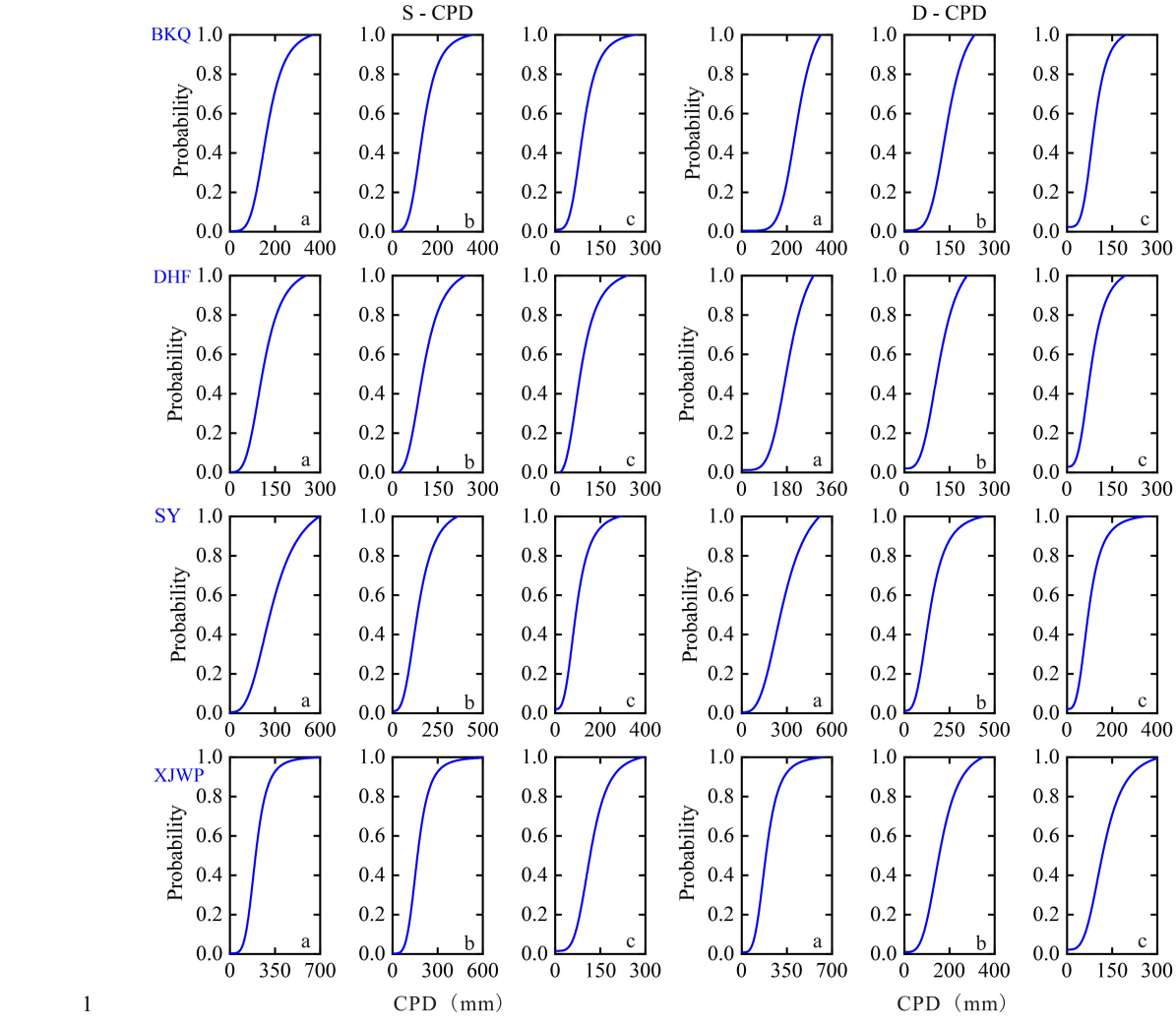

Figure. 9 Conditional probabilities of occurrence of moderate (a), severe (b), and extreme (c) hydrological drought under the circumstance of various CPD at HRB.

5 Conclusions

In this paper, SPI and SRI were adopted to characterize meteorological and hydrological drought respectively, and the spatiotemporal variation characteristics of hydrological drought were identified in the HRB from 1967 to 2019. Meanwhile, copula functions were established based on drought duration and severity to calculate the return period of hydrological drought. Furthermore, the PTMH were determined by calculating the Pearson correlation coefficients between 1-month SRI and multi-time scale SPI. Finally, based on CPD thresholds for triggering hydrological drought, the impact of large reservoir on drought resistance of the basin was revealed. From the results, primary conclusions are given as follows:

(1) Hydrological drought showed a slight strengthening trend in DHF, while presented alternate characteristics of drought

https://doi.org/10.5194/nhess-2021-218
Preprint. Discussion started: 21 July 2021

and flood in SY and XJWP from 1967 to 2019. From seasonal perspective, drought presented an strengthening trend in each season at DHF. Nevertheless, drought presented an strengthening trend in summer and autumn, while showed a decreasing trend in spring and winter at SY and XJWP.

(2) The western and center of the HRB were vulnerable districts to hydrological drought with longer drought duration and higher severity. Furthermore, the eastern region of the HRB was more sensitive to short-duration drought, which was dominated by two-month and three-month drought events.

(3) The return periods T_{and} (T_{or}) of moderate, severe, and extreme hydrological drought in DHF, SY and XJWP were 2.3 (1.7), 4.5 (3.1), 22.8 (14.9), 3.3 (2.7), 6.7 (4.8), 71.0 (18.6), 3.2 (2.6), 7.3 (4.4) and 79.0 (16.3) years, respectively.

(4) The average PTMH in BKQ, DHF, SY and XJWP were 4.1, 4.3, 14.9, and 1.9 months, respectively, which indicated that the PTMH of the lower reaches of DHF reservoir has been significantly improved owing to the operation of DHF. Moreover, with the increase of interval between hydrological station and DHF reservoir, the improvement effect was weakened.

(5) The mean CPD thresholds at BKQ, DHF, SY and XJWP were 172.1, 169.8, 211.2 and 230.9 mm, severe were 236.0, 192.8, 302.6 and 315.5 mm, and extreme were 324.3, 249.8, 518.3 and 391.3 mm, respectively, which showed that the operation of large reservoir strengthened the drought resistance in the lower reaches while lightly weaken the drought resistance in the upper reaches of DHF reservoir.

Generally, the findings of this study are helpful to reveal the evolution characteristics of hydrological drought and the efficiency of large reservoir in resisting drought. Therefore, the establishment of drought hydrological warning and control system based on the operation of large reservoirs is of certain practical value to the local drought mitigation.

Data availability. Some or all data, models, or code that support the findings of this study are available from the corresponding author upon reasonable request.

Author Contribution. Conceptualization: S P.Y; F T.Y. Methodology: F T.Y; S P.Y; X D.S. Data gather: X D.S; S P.Y. Formal analysis and investigation: S P.Y; X D.S; F T.Y. Writing manuscript: S P.Y; F T.Y.

Conflicts of interest. The authors declare that they have no known competing financial interests or personal relationships that could have appeared to influence the work reported in this paper.

https://doi.org/10.5194/nhess-2021-218
Preprint. Discussion started: 21 July 2021

References

- Barker, L. J., Hannaford, J., Chiverton, A., and Svensson, C.: From meteorological to hydrological drought using standardised indicators, Hydrol. Earth Syst. Sci., 20, 2483–2505, https://doi.org/10.5194/hess-20-2483-2016, 2016.
- Beniston, M., and Stephenson, D.B.: Extreme climatic events and their evolution under changing climatic conditions, Glob. Planet. Change., 44, 1-9, https://doi.org/10.1016/j.gloplacha.2004.06.001, 2004.
- Chang, J., Guo, A., Wang, Y., Ha, Y., Zhang, R., Xue, L., and Tu, Z.: Reservoir operations to mitigate drought effects with a hedging policy triggered by the drought prevention limiting water level, Water Resour. Res., 55, 904-922, https://doi.org/10.1029/2017WR022090, 2019.
- Chen, X., Li, F.W., and Feng, P.: Spatiotemporal variation of hydrological drought based on the Optimal Standardized Streamflow Index in Luanhe River basin, China, Nat. Hazards., 91, 155-178, https://doi.org/10.1007/s11069-017-3118-6, 2018.
- Christensen, O.B., and Christensen, J.H.: Intensification of extreme European summer precipitation in a warmer climate, Global Planet. Change., 44, 107-117, https://doi.org/10.1016/j.gloplacha.2004.06.013, 2004.
- Dash, S.S., Sahoo, B., and Raghuwanshi, N.S.: A SWAT-Copula based approach for monitoring and assessment of drought propagation in an irrigation command, Ecol. Eng., 127, 417- 430, https://doi.org/10.1016/j.ecoleng.2018.11.021, 2019.
- Fang, W., Huang, S., Huang, Q., Huang, G., Wang, H., Leng, G., Wang, L., and Guo, Y.: Probabilistic assessment of remote sensing-based terrestrial vegetation vulnerability to drought stress of the Loess Plateau in China, Remote Sens. Environ., 232, 111292, https://doi.org/10.1016/j.rse.2019.111290, 2019.
- Gevaert, A.I., Veldkamp, T.I.E., and Ward, P.J.: The effect of climate type on timescales of drought propagation in an ensemble of global hydrological models, Hydrol. Earth Syst. Sci., 22, 4649-4665, https://doi.org/10.5194/hess-22-4649-2018, 2018.
- Guo, Y., Huang, Q., Huang, S.Z., Leng, G.Y., Zheng, X.D., Fang, W., Deng, M.J., and Song, S.B.: Elucidating the effects of mega reservoir on watershed drought tolerance based on a drought propagation analytical method, J. Hydrol., PP, 125738, https://doi.org/10.1016/j.jhydrol2020.125738, 2020.
- Guo, Y., Huang, S.Z., Huang, Q., Leng, G.Y., Fang, W., Wang, L., and Wang, H.: Propagation thresholds of meteorological drought for triggering hydrological drought at various levels, Science of The Total Environment., 712, 136502, https://doi.org/10.1016/j.scitotenv.2020.136502, 2020.
- Guo, Y., Huang, S.Z., Huang, Q., Wang, H., Fang, W., Yang, Y.Y., and Wang, L.: Assessing socioeconomic drought based on an improved multivariate standardized reliability and resilience index, J. Hydrol., 568, 904-918, https://doi.org/10.1016/j.jhydrol.2018.11.055, 2019.

https://doi.org/10.5194/nhess-2021-218
Preprint. Discussion started: 21 July 2021

- Huang, S.Z., Chang, J.X., Leng, G.Y., and Huang, Q.: Integrated index for drought assessment based on variable fuzzy set theory: a case study in the Yellow River basin, China, J. Hydrol., 527, 608-618, https://doi.org/10.1016/j.jhydrol.2015.05.032, 2015.
- Huang, W.C., and Chou, C.C.: Risk-based drought early warning system in reservoir operation, Adv. Water Resour., 31, 649-660, https://doi.org/10.1016/j.advwatres.2007.12.004, 2008.
- Kao, S.C., and Govindaraju, R.S.: A copula-based joint deficit index for droughts, J. Hydrol., 380 (1-2), 121-134, https://doi.org/10.1016/j.jhydrol.2009.10.029, 2009.
- Kim, S., Kim, B., Ahn, T.J., and Kim, H.S.: Spatio-temporal characterization of Korean drought using severity-area-duration curve analysis, Water Environ. J., 25 (1), 22-30, https://doi.org/10.1111/j.1747-6593.2009.00184.x, 2011.
- Kunkel, K.E.: North American trends in extreme precipitation, Nat. Hazards., 29, 291-305, https://doi.org/10.1023/A:1023694115864, 2003.
- Lee, T., Modarres, R., and Ouarda, T.B.M.J.: Data-based analysis of bivariate copula tail dependence for drought duration and severity, Hydrol. Processes., 27, 1454-1463, https://doi.org/10.1002/hyp.9233, 2013.
- Leng, G.Y., Tang, Q.H., and Rayburg, S.: Climate change impacts on meteorological, agricultural and hydrological droughts in China, Global Planet. Change., 126, 23-34, https://doi.org/10.1016/j.gloplacha.2015.01.003, 2015.
- Lindenschmidt, K.E., and Rokaya, P.: A stochastic hydraulic modelling approach to determining the probable maximum staging of Ice-Jam floods, J. Environ. Informatics., 34 (1), 45-54, https://doi.org/10.3808/jei.201900416, 2019.
- Liu, Z.P., Wang, Y.Q., Shao, M.G., Jia, X.X ., and Li, X.L.: Spatiotemporal analysis of multiscalar drought characteristics across the Loess Plateau of China, J. Hydrol., 534, 281-299, https://doi.org/10.1016/j.jhydrol.2016.01.003, 2016a.
- Liu, Z.Y., Menzel, L., Dong, C.Y., and Fang, R.H.: Temporal dynamics and spatial patterns of drought and the relation to ENSO: A case study in Northwest China, Int. J. Climatol., 36 (8), 2886-2898, https://doi.org/10.1002/joc.4526, 2016b.
- Lorenzo-Lacruz, J., Vicente-Serrano, S.M., González-Hidalgo, J.C., López-Moreno, J.I., and Cortesi, N.: Hydrological drought response to meteorological drought in the Iberian Peninsula, Clim. Res., 58, 117-131, https://www.jstor.org/stable/24896134, 2013.
- McKee, T.B.N., Doesken, J., and Kleist, J.: The relationship of drought frequency and duration to time scales, In: Eight Conf. On Applied Climatology, Anaheim, CA, Amer. Meteor. Soc., pp, 179-184, 1993.
- Mirabbasi, R., Fakheri-Fard, A., and Dinpashoh, Y.: Bivariate drought frequency analysis using the copula method, Theor. Appl. Climatol., 108 (1-2), 191-206, https://doi.org/10.1007/s00704-011-0524-7, 2012.

https://doi.org/10.5194/nhess-2021-218
Preprint. Discussion started: 21 July 2021

- Mishra, A.K., and Singh, V.P.: Drought modelling – a review. J. Hydrol., 403, 157-175, https://doi.org/10.1016/j.jhydrol.2011.03.049, 2011.
- Oladipo, E.O.: A comparative performance analysis of three meteorological drought indices, J. Clim., 5, 655–664, https://doi.org/10.1002/joc.3370050607, 1985.
- Palmer, T.N., and Räisänen, J.: Quantifying the risk of extreme seasonal precipitation events in a changing climate, Nature., 415, 512-514, https://doi.org/10.1038/415512a, 2002.
- Pandey, R.P., and Ramasastri, K.S.: Relationship between the common climatic parameters and average drought frequency, Hydrol. Processes., 15, 1019-1032, https://doi.org/10.1002/hyp.187, 2001.
- Rivera, J.A., Penalba, O.C., Villalba, R., and Araneo, D.C.: Spatio-temporal patterns of the 2010-2015 extreme hydrological drought across the Central Andes, Argentina, Water., 9, 652, https://doi.org/10.3390/w9090652, 2017.
- Sattar, M.N., Lee, J.Y., Shin, J.Y., and Kim, T.W.: Probabilistic characteristics of drought propagation from meteorological to hydrological drought in South Korea, Water Resour. Manag., 33, 2439-2452, https://doi.org/10.1007/s11269-019-02278-9, 2019.
- Shiklomanov, I.A., Shiklomanov, A.I., Lammers, R.B., Peterson, B.J., and Vorosmarty, C.J.: The dynamics of river water inflow to the arctic ocean, Freshw. Budget Arctic Ocean., 281-296, https://doi.org/10.1007/978-94-011-4132-1_13, 2000.
- Sun, S.L., Li, Q., Li, J., and Wang, G.: Revisiting the evolution of the 2009-2011 meteorological drought over Southwest China, J. Hydrol., 568, 385-402, https://doi.org/10.1016/j.jhydrol.2018.10.071, 2019.
- Van Loon, A.F., Van Huijgevoort, M.H.J., and Van Lanen, H.A.J.: Evaluation of drought propagation in an ensemble mean of large-scale hydrological models, Hydrol. Earth Syst. Sci., 16, 4057-4078, https://doi.org/10.5194/hess-16-4057-2012, 2012.
- Vicente-Serrano, S.M., López-Moreno, J.I., Beguería, S., Lorenzo-Lacruz, J., AzorinMolina, C., and Morán-Tejeda, E.: Accurate computation of a streamflow drought index, J. Hydrol. Eng., 17, 318-332, https://doi.org/10.1061/(ASCE)HE.1943-5584.0000433, 2012.
- Vyver, H.V.D., and Bergh, J.V.D.: The Gaussian copula model for the joint deficit index for droughts, J. Hydrol., 561, 987-999, https://doi.org/10.1016/j.jhydrol.2018.03.064, 2018.
- Wang, F., Wang, Z.M., Yang, H.B., Di, D.Y., Zhao, Y., Liang, Q.H., and Hussain, Z.: Comprehensive evaluation of hydrological drought and its relationships with meteorological drought in the Yellow River basin, China, J. Hydrol., 584, 124751, https://doi.org/10.1016/j.jhydrol.2020.124751, 2020.
- Wang, Y.M., Yang, J., Chang, J.X., and Zhang, R.: Assessing the drought mitigation ability of the reservoir in the downstream of the Yellow River, Sci. Total Environ., 646, 1327-1335, https://doi.org/10.1016/j.scitotenv.2018.07.316, 2019.

https://doi.org/10.5194/nhess-2021-218
Preprint. Discussion started: 21 July 2021

- Wilhite, D.A., and Glantz, M.H.: Understanding: the drought phenomenon: the role of definitions, Water Int., 10, 111-120, https://doi.org/10.1080/02508068508686328, 1985.
- Wu, J.F., Chen, X.W., Gao, L., Yao, H.X., Chen, Y., Liu, and M.B., Shukla, S.: Response of hydrological drought to meteorological drought under the influence of large reservoir, Adv. Meteorol., 2016, 1-11, https://doi.org/10.1155/2016/2197142, 2016.
- Wu, J.F., Chen, X.W., Yao, H.X., Gao, L., Chen, Y., and Liu, M.B.: Non-linear relationship of hydrological drought responding to meteorological drought and impact of a large reservoir, J. Hydrol., 551, 495-507, https://doi.org/10.1016/j.jhydrol.2017.06.029, 2017.
- Wu, J.F., Liu, Z.Y., Yao, H.X., Chen, X.H, Chen, X.W, Zheng, Y.H., and He, Y.H.: Impacts of reservoir operations on multi-scale correlations between hydrological drought and meteorological drought, J. Hydrol., 563, 726-736, https://doi.org/10.1016/j.jhydrol.2018.06.053, 2018.
- Xu, K., Yang, D.W., Xu, X.Y., and Lei, H.M.: Copula based drought frequency analysis considering the spatio-temporal variability in Southwest China, J. Hydrol., 527, 630-640, https://doi.org/10.1016/j.jhydrol.2015.05.030, 2015.
- Xu, Y., Zhang, X., Wang, X., Hao, Z.C., Singh, V.P., and Hao, F.H.: Propagation from meteorological drought to hydrological drought under the impact of human activities: a case study in northern China, J. Hydrol., 579, 124147, https://doi.org/10.1016/j.jhydrol.2019.124147, 2019.
- Yang, X., Li, Y.P., Liu, Y.R., and Gao, P.P.: A MCMC-based maximum entropy copula method for bivariate drought risk analysis of the Amu Darya River Basin, J. Hydrol., 590, 125502, https://doi.org/10.1016/j.jhydrol.2020.125502, 2020.
- Zhao, P.P., Lu, H.S., Fu, G.B., Zhu, Y.H., Su, J.B., and Wang, J.Q.: Uncertainty of hydrological drought characteristics with copula functions and probability distributions: a case study of Weihe River, China, Water., 9 (5), 334, https://doi.org/10.3390/w9050334, 2017.